

Stereochemical Systematics of Metal Clusters. Structural Characterization of a Genuine One-Electron Metal–Metal Bonded Cobalt Dimer $[(\eta^5\text{-C}_5\text{H}_5)\text{CoP}(\text{C}_6\text{H}_5)_2]_2^+$ and Related Compounds by Extended X-Ray Absorption Fine Structure Spectroscopy

Boon-Keng Teo,* P. Eisenberger, and B. M. Kincaid

Contribution from the Bell Laboratories, Murray Hill, New Jersey 07974.

Received June 15, 1977

Abstract: Application of extended x-ray absorption fine structure (EXAFS) spectroscopy to the chemically unstable, first “genuine” “one-electron” metal–metal bonded cobalt dimer $[\text{CpCoPPh}_2]_2^+$ provides strong structural evidence that the metal–metal bond weakens significantly upon oxidation from the neutral to the monocationic species. This is consistent only with the theory that the electron being removed comes from an orbital which is highly bonding between the two cobalt atoms. Rather unexpectedly, however, the cobalt–cobalt distance increases by only 0.08 Å in going from the neutral compound (2.57 Å) to its monocation (2.65 Å). It is concluded that the stereochemical influence on metal framework imposed by varying the number of metal cluster electrons decreases drastically in going from antibonding to bonding to (or) nonbonding orbitals (with respect to metal–metal interactions). The metal–ligand and metal–metal (if any) distances of cobaltocene and the series of phosphido-bridged cobalt dimers with the general formula $[\text{CpCoPPh}_2]_2(\text{OH})_m^n$ (where $m = 0, n = 0, +1; m = 1, n = +1; \text{Cp} = \eta^5\text{-C}_5\text{H}_5$; and $\text{Ph} = \text{C}_6\text{H}_5$) have also been determined by this technique. The weak metal–metal contributions to the EXAFS spectra of the dimeric species necessitate the development of a difference-Fourier technique in the data analysis.

Introduction

The stereochemical influence of valence electrons on metal cluster systems has been the subject of many recent studies.^{1–10} Oxidation(s) of metal–metal *nonbonded* systems such as *cis*- $[\text{CpFe}(\text{CO})\text{PPh}_2]_2^n$ ($n = 0, +1, +2$)³ and *cis*- $[\text{CpFeYSR}]_2^n$ ($\text{Y} = \text{CO}, \text{R} = \text{Ph}, n = 0; \text{Y} = \text{CO}, \text{R} = \text{Me}, n = +1; \text{Y} = \text{NCCH}_3, \text{R} = \text{Et}, n = +2; \text{Cp} = \eta^5\text{-C}_5\text{H}_5; \text{Ph} = \text{C}_6\text{H}_5$)^{4a–c} have been shown to cause a stepwise decrease in metal–metal distance from a nonbonding (3.498 (4), 3.39 Å) in the neutral species to a half-bonding (3.14 (2), 2.925 (4) Å) in the monocations to a bonding (2.764 (4), 2.649 (7) Å) value in the dications. These tremendous decreases in metal–metal distance only were rationalized by the stepwise removal of two electrons from the highly metal–metal antibonding orbital. In a simplified two-level approximation for these dimers, the number of “metal cluster electrons” (viz., the number of electrons primarily responsible for metal–metal interactions) decreases from four (two in the bonding a_1 , and two in the antibonding b_2^* orbital, $a_1^2b_2^{*2}$, under C_{2v} symmetry) to three ($a_1^2b_2^{*1}$) to two ($a_1^2b_2^{*0}$) for $n = 0, +1, +2$ in these iron dimers.² Reductions of metal–metal systems such as $\text{M}_2(\text{CO})_6(\text{PMe}_2)_2^n$ ($\text{M} = \text{Fe}, \text{Ru}; n = 0, -1, -2; \text{Me} = \text{CH}_3$) and $\text{M}_2(\text{CO})_8(\text{PMe}_2)_2^n$ ($\text{M} = \text{Cr}, \text{Mo}, \text{W}; n = 0, -1, -2$) have also been reported.⁵ Though no structural information is available, extensive spectroscopic data suggest that the metal–metal distance increases upon stepwise reduction. This is again in accord with the two-level model in that the antibonding metal–metal orbital is successively populated with one and two electrons upon reduction, resulting in the electronic configurations of $a_1^2b_2^{*0}$, $a_1^2b_2^{*1}$, and $a_1^2b_2^{*2}$ for $n = 0, -1, -2$ for these latter systems.

In contrast, the stereochemical consequences of the oxidation of metal–metal bonded systems are less obvious. The tetramercapto-bridged dimer $\text{Cp}_2\text{Mo}_2(\text{SMe})_4$ which has a single Mo–Mo bond has been oxidized by one electron to yield the monocation. Structural characterizations revealed only a small increase in the Mo–Mo distance, going from 2.603 (2) Å in the neutral to 2.617 (4) Å in the monocationic species.⁶ Both of these values are, however, within the bonding range.

In view of this uncertainty as well as the recent controversy

over the relationship, if any, between metal–metal distance and the degree of metal–metal bonding,⁷ we decided to perform a structural determination on the “genuine” “one-electron” metal–metal bonded ($a_1^1b_2^{*0}$) system $[\text{CpCoPPh}_2]_2^+$ ⁸ by extended x-ray absorption fine structure (EXAFS) spectroscopy.^{11–25}

This paper reports the analysis of the EXAFS spectra of cobaltocene and a series of phosphido-bridged cobalt dimers with the general formula $[\text{CpCoPPh}_2]_2(\text{OH})_m^n$ (where $m = 0, n = 0, +1; m = 1, n = +1; \text{Cp} = \eta^5\text{-C}_5\text{H}_5$; and $\text{Ph} = \text{C}_6\text{H}_5$). The neutral compound has a bonding Co–Co distance of 2.56 (1) Å.⁹ Attempts to determine the Co–Co distance in the monocation by single-crystal x-ray diffraction have led to the diamagnetic $[\text{CpCoPPh}_2]_2\text{OH}^+$ cation (owing to its sensitivity toward moisture in the crystal growing process) which has a Co···Co distance of 2.90 (1) Å.⁸ To our surprise, the EXAFS spectroscopy (described herein) indicates a significant weakening (as determined by a nearly twofold increase in Debye–Waller factor) in the cobalt–cobalt bond upon oxidation but only a relatively small increase in the cobalt–cobalt distance from 2.56 Å in the neutral to 2.65 Å in the monocation.

EXAFS Spectroscopy

Two major developments have recently been advanced which make EXAFS a highly attractive structural tool. The first is the formulation and the understanding of the physics involved.^{11–16} The oscillatory part of the x-ray absorption rate (μ) of a particular element beyond its absorption edge (e.g., K edge) is given by

$$\chi(k) = \frac{\mu - \mu_0}{\mu_0} = \frac{1}{k} \sum_i N_i F_i(k) e^{-2\sigma_i^2 k^2} \times \frac{\sin(2kr_i + \phi_i(k))}{r_i^2} \quad (1)$$

where μ_0 is the atomic absorption cross section, $F_i(k)$ is the backscattering amplitude from each of the N_i neighboring atoms of the i th kind with a Debye–Waller factor σ_i (which includes both thermal vibration and static disorder) at a distance r_i away, and $\phi_i(k)$ is the phase shift experienced by the

outgoing and the backscattered photoelectron due to the absorber and the i th scatterer, respectively. The variable k is the photoelectron wavevector which is related to the photon energy E by

$$k = \sqrt{\frac{2m}{\hbar^2} (E - E_0)} \quad (2)$$

where E_0 is the energy threshold for an electron ejected from the absorbing atom. It is apparent from eq 1 and 2 that if we know the amplitude $F_i(k)$ and the phase $\phi_i(k)$ functions we can determine not only the interatomic distances r_i but also the Debye-Waller factors σ_i and, under favorable conditions, the number of atoms N_i .¹⁶⁻²⁵ It should be mentioned that the Debye-Waller factor as determined by EXAFS spectroscopy is different from that implied by the conventional crystallography in that it refers to the root mean square relative vibrational amplitude between two atoms *along the bond direction* and not the absolute root mean square displacement of individual atoms. The second major development is the availability of synchrotron radiation at Stanford Synchrotron Radiation Laboratory (SSRL) which greatly improves the signal to noise ratio by $\sim 10^5$ over the conventional x-ray sources.^{15,24} The real attractiveness of this technique, however, lies in its structural application to complex biological or chemical systems where single crystals are not available (viz., polymeric or amorphous solid, liquid, solution, gas, etc.).

The accuracy of EXAFS structural determination depends on two factors. First, in order to measure interatomic distances and Debye-Waller factors accurately, the phase shift and the amplitude functions (respectively) must be to a large extent insensitive to chemical environment and thus can be transferred from one chemical system to another. Indeed this has been demonstrated to be the case.^{17c,19,20,25} Secondly, the phase $\phi(k)$ and the amplitude $F(k)$ information must be either predetermined empirically from model compounds^{17,19,20-22} or calculated theoretically from first principles.¹²⁻¹⁵ While both approaches have met with significant success, we note that the recent theory of Lee and Beni¹⁴ on EXAFS amplitude and phase functions has been shown to provide interatomic distances accurate to ± 0.01 Å and Debye-Waller factors accurate to $\pm 10\%$ (in single distance systems). Subsequent parameterization of these theoretical functions with simple analytical forms provide a set of working parameters which can be used for curve fitting of EXAFS spectra.^{25a,b}

Experimental Section

Materials. All reactions were carried out under an argon atmosphere. Dichloromethane and toluene were carefully dried and freshly distilled from P_2O_5 before use. The products were stored and handled in a drybox.

Cobaltocene (**1**) was purchased from Strem Chemicals and used without further purification.

Following Hayter's method,¹⁰ $[CpCoPPh_2]_2$ (**2**) was prepared from the reaction of $CpCo(CO)_2$ with P_2Ph_4 in toluene and purified via recrystallization from toluene. The purity of the product was checked by infrared spectroscopy and elemental analysis.

The monocation $[CpCoPPh_2]_2^+PF_6^-$ (**3**) was prepared from the quantitative reaction of $[CpCoPPh_2]_2$ with $AgPF_6$ in freshly prepared, dried, and deoxygenated dichloromethane according to the known method.⁸ The monocation was confirmed by elemental analysis and infrared and electron paramagnetic spectroscopies. The latter exhibits at room temperature the highly characteristic well-resolved 31-hyperfine-line EPR spectrum⁸ with a g value of 2.035 and an intensity pattern of 1:2:3...16...3:2:1.

The monocation $[CpCoPPh_2]_2^+PF_6^-$ in CH_2Cl_2 was then allowed to react with a small amount of water for 20 min. The reaction mixture was subsequently rotavaced to give an unknown mixture of $[CpCoPPh_2]_2^+PF_6^-$ and $[CpCoPPh_2]_2OH^+PF_6^-$ (**4**). The known structure⁸ of the diamagnetic $[CpCoPPh_2]_2OH^+PF_6^-$ serves as an "internal" standard for the determination of the distance of the ex-

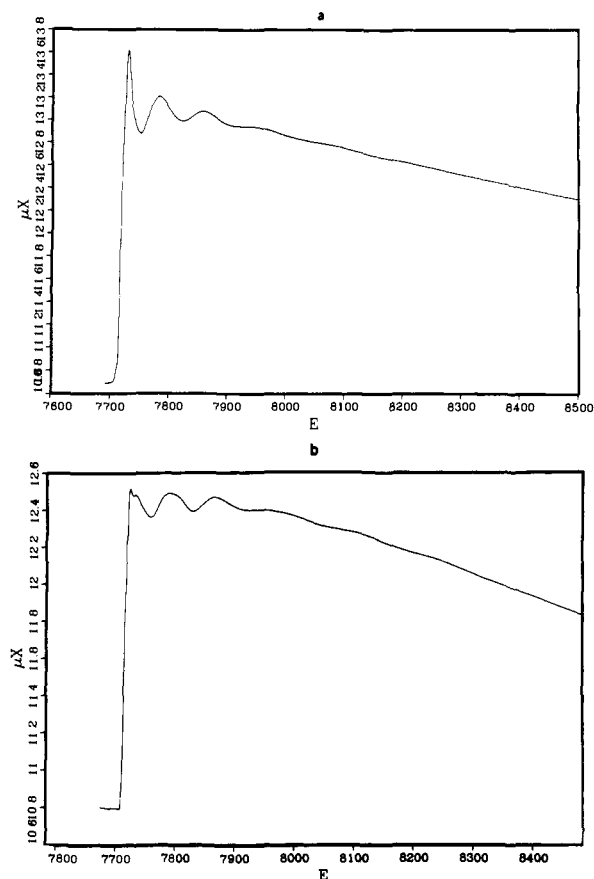


Figure 1. X-ray absorption spectra (Co K edge) of cobaltocene (a) and $[CpCoPPh_2]_2$ (b).

pectedly weak cobalt-cobalt bond in the paramagnetic $[CpCoPPh_2]_2^+PF_6^-$.

All spectra were run as a compressed neat solid pellet ($x \times 2 \times 40$ mm³ where the thickness x is typically 1.5 mm) loaded in a drybox and sealed with thin Kapton tape. The cells were kept under an inert atmosphere until just prior to measurements.

X-Ray Absorption Measurements. All x-ray absorption measurements described herein were performed at Stanford Synchrotron Radiation Laboratory (SSRL) using the synchrotron radiation from Stanford Positron Electron Accelerating Ring (SPEAR).²⁶ The spectrometer used was EXAFS I originally constructed by Kincaid, Eisenberger, and Sayers which has been described elsewhere.²⁷ The x-ray beam (slit = 1×20 mm²) from SPEAR, after being monochromated by a channel-cut [220] silicon crystal, passes through first one ionization chamber which measures the incident beam intensity I_0 , then the sample, and finally another ionization chamber which measures the transmitted intensity I . Nitrogen was the detecting gas used in both ionization chambers. The EXAFS spectra were typically recorded with an integration time of 2 s/point with 400 steps covering about 800 eV above the edge.

Data Analysis

Data Reduction. Figures 1a and 1b show typical plots of $\mu x = \ln(I_0/I)$ as a function of x-ray photon energy E at and above the K edge of cobalt for Cp_2Co (**1**) and $[CpCoPPh_2]_2$ (**2**), respectively. For the EXAFS analysis, it is necessary to plot the normalized fine structure $\chi(k) = (\mu - \mu_0)/\mu_0$ as a function of the photoelectron wavevector

$$k = \sqrt{\frac{2m}{\hbar^2} (E - E_0)}$$

Since we will be using theoretical amplitude and phase functions in the following analysis which necessitate the least-squares refinement of the energy threshold E_0 (viz., an arbitrarily chosen experimental E_0 may not be consistent with theoretical phase shifts),^{14,25} we choose a reasonable E_0 of

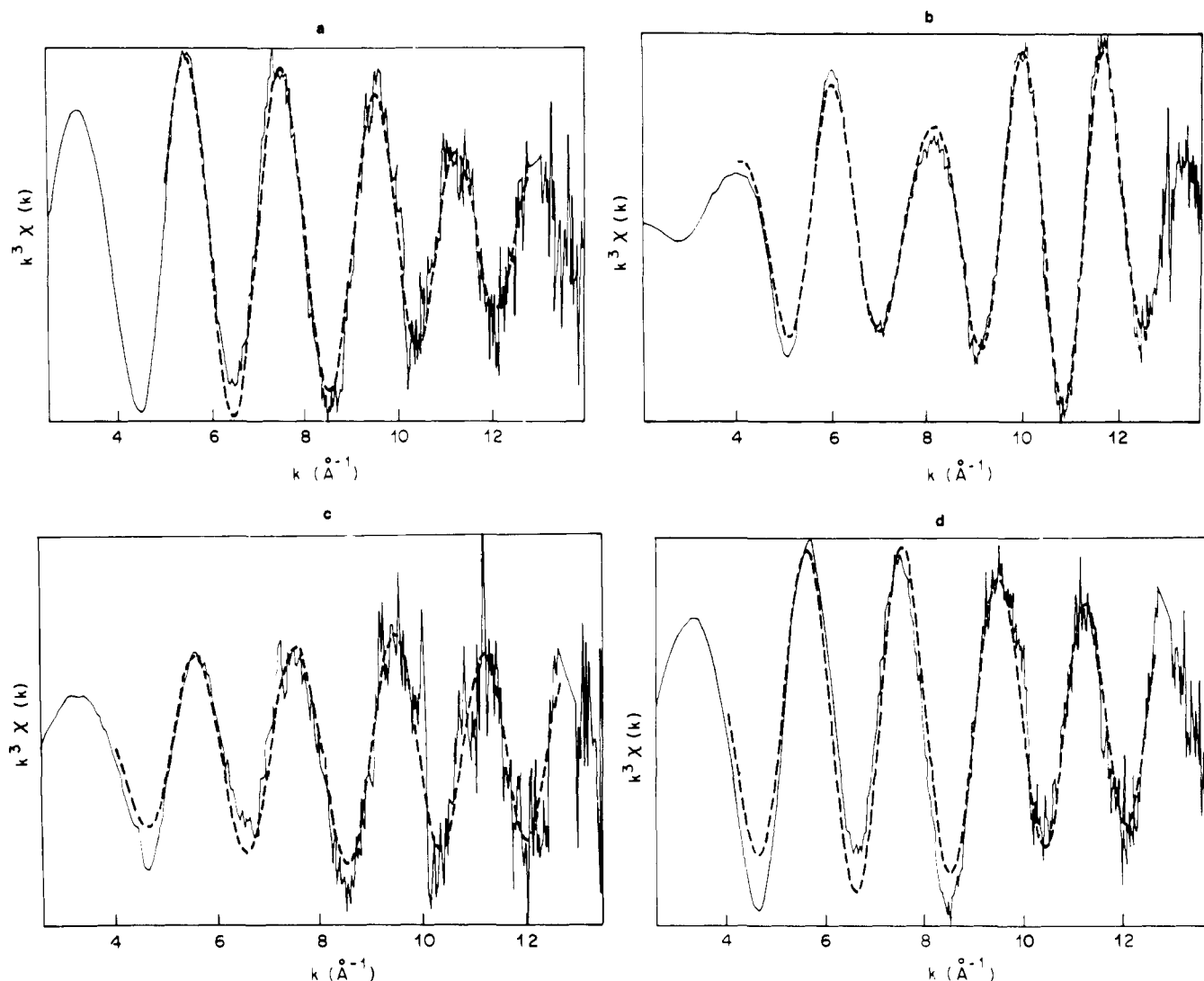


Figure 2. Unfiltered (solid curves) and Fourier filtered (dashed curves) $\chi(k)k^3$ vs. k EXAFS data: (a) Cp_2Co ; (b) $[\text{CpCoPPH}_2]_2$; (c) $[\text{CpCoPPH}_2]_2^+$; (d) $[\text{CpCoPPH}_2]_2^+ / [\text{CpCoPPH}_2]_2\text{OH}^+$. The ordinate scales are (a) -2.86 to 2.79 ; (b) -6.40 to 5.88 ; (c) -9.06 to 10.71 ; and (d) -7.73 to 6.64 \AA^{-3} .

7750 eV for all compounds studied. After conversion to k space in \AA^{-1} , the data were multiplied by k^3 and the background—a large part of which is due to the ligand absorption as well as the effect that the ionization chamber efficiency changes with photon energy—was removed by using a cubic spline technique (three sections with $\Delta k = 4 \text{ \AA}^{-1}$ each).^{28a} The $\chi(k)k^3$ vs. k data were then corrected for the μ_0 dropoff via Victoreen's true $\mu_0/\rho = C\lambda^3 - D\lambda^4$ equation with $C = 141$, $D = 33.2$ for cobalt.²⁹ The resulting curves (solid) are shown in Figures 2(a)–(d).

For the purpose of curve fitting, the high frequency noise and the residual background in each spectrum were further removed by a Fourier filtering technique.^{28b} It involves Fourier transforming the $\chi(k)k^3$ data into R space, selecting the distance (R) range to be kept, and back transforming to k space. The Fourier transforms of the data in Figures 2(a)–(d) are depicted in Figures 3(a)–(d), respectively. Smooth filtering windows of 0.8–3.0, 0.8–3.2, 0.8–3.4, and 0.8–3.4 \AA were used for 1, 2, 3, and 4, respectively. The resulting filtered data, subsequently truncated at ~ 4 and 12.6 \AA^{-1} , are compared (dashed vs. solid curves) with the unfiltered data in Figures 2(a)–(d). These filtered data were used for the following curve fitting.

Least-Squares Refinements. We use the least-squares minimization technique to fit the filtered spectra with a mul-

tiple-term semiempirical expression of the EXAFS model. A nonlinear least-squares program, which utilizes Marquardt's scheme for iterative estimation of nonlinear least-squares parameters via a compromise combination of gradient (when far from minimum) and Taylor series (when close to a minimum) method, was used.³⁰ For $[\text{CpCoPPH}_2]_2$ which contains three different types of nearest neighbors (viz., five cyclopentadienyl carbon, two phosphorus, and one cobalt atoms), a three-term fit of the following expression must be used.

$$\chi(k)k^3 = N \left\{ N_{\text{C}}F_{\text{C}}(k_{\text{C}})e^{-2\sigma_{\text{C}}^2k^2}k_{\text{C}}^2 \times \frac{\sin(2k_{\text{C}}r_{\text{C}} + \phi_{\text{C}}(k_{\text{C}}))}{r_{\text{C}}^2} + N_{\text{P}}F_{\text{P}}(k_{\text{P}})e^{-2\sigma_{\text{P}}^2k^2}k_{\text{P}}^2 \times \frac{\sin(2k_{\text{P}}r_{\text{P}} + \phi_{\text{P}}(k_{\text{P}}))}{r_{\text{P}}^2} + N_{\text{Co}}F_{\text{Co}}(k_{\text{Co}})e^{-2\sigma_{\text{Co}}^2k^2}k_{\text{Co}}^2 \times \frac{\sin(2k_{\text{Co}}r_{\text{Co}} + \phi_{\text{Co}}(k_{\text{Co}}))}{r_{\text{Co}}^2} \right\} \quad (3)$$

The terms $F_i(k_i)$, $\phi_i(k_i)$, N_i , σ_i , r_i , and k_i denote the amplitude, the phase, the number of bonds, the Debye-Waller fac-

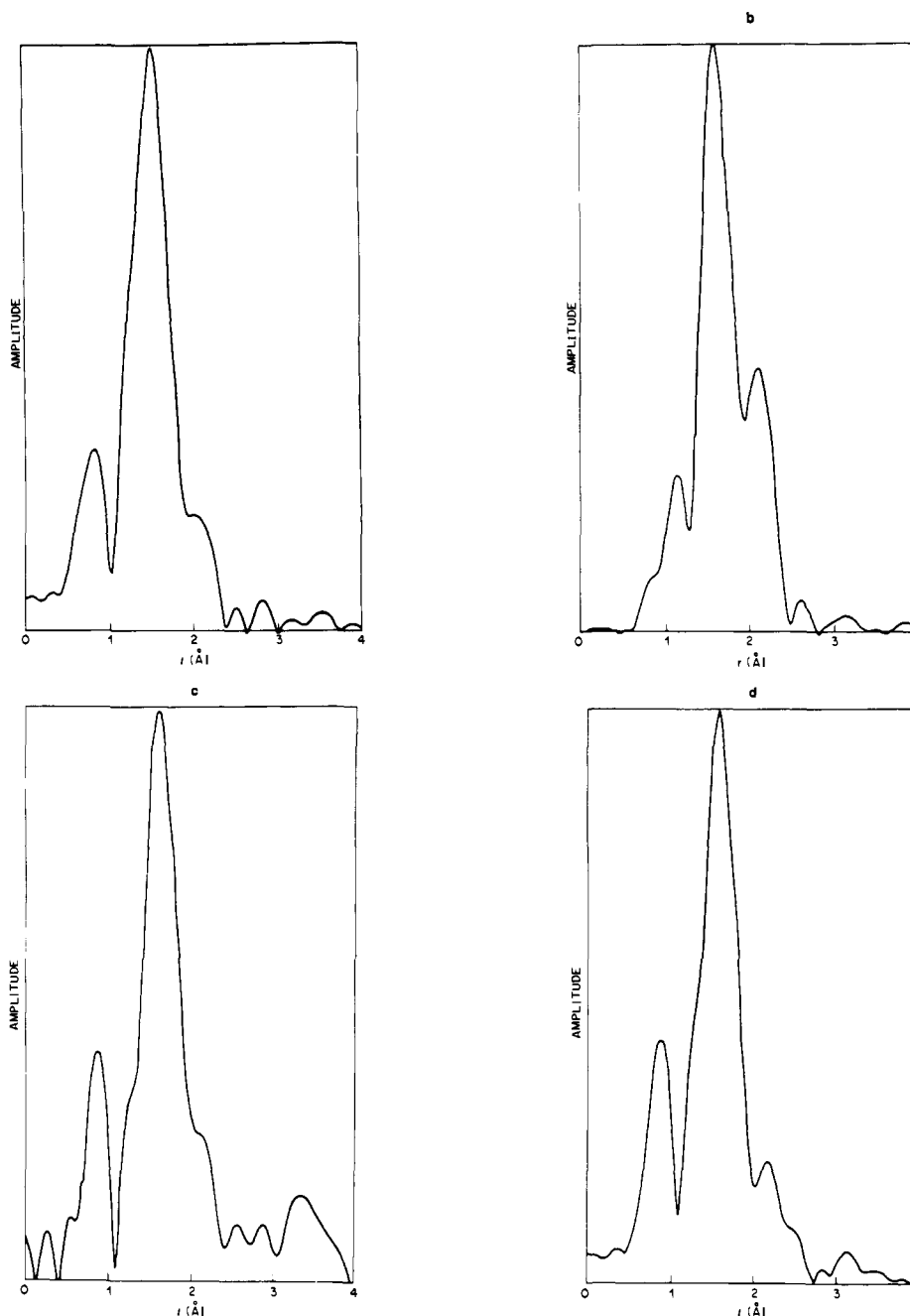


Figure 3. Fourier transforms of the unfiltered EXAFS data shown in Figure 2. The ordinate scales are (a) 0-124; (b) 0-237; (c) 0-290; and (d) 0-309 \AA^{-4} .

tor, the bond distance, and the photoelectron wavevector, respectively, of the i th type neighboring atoms where $i = \text{C, P, Co}$. For such a complex system, it has been found impractical to vary the overall scale factor N , the amplitude functions, the number of bonds, the Debye-Waller factors, and the distances simultaneously even with a detailed knowledge of phase shifts. The reason is that significant correlations can occur within and between the two sets of functions $\{\phi(k), E_0, r\}$ and $\{F(k), \sigma, N\}$ of each term as well as between different scattering terms. It is obvious that strong correlations can render the individual parameters nonunique and/or result in false minima in curve fitting. Empirically, one can obtain (1) the amplitude function by curve fitting the EXAFS spectrum of a model compound (preferably a single-term system) with a known structure by fixing the coordination number and the Debye-Waller factor (either known or reasonably assumed; in the latter case, all the Debye-Waller factors determined subsequently for the un-

known compounds will be *relative* to that assumed for the model compound) and (2) the phase shifts by holding the known distance fixed. These functions can then be transferred to unknown systems analyzed in a similar fashion (such as background removal, cutoffs of data, Fourier filtering, etc., so as to minimize systematic errors) in order to determine the number of bonds and/or Debye-Waller factors as well as the interatomic distances. This procedure works reasonably well for most systems. However, for multiatom, multidistance systems with (1) more than two or three contributions from scatterers of similar (or identical) atomic numbers and similar distances; (2) one term dominating the EXAFS spectrum; (3) unknown bond type and/or bond numbers and unknown Debye-Waller factors, care must be taken to ensure the validity or significance of the resulting parameters. In the first case, trading of the amplitudes between different terms and/or between the amplitudes and the distances can occur. One in-

Table I. Theoretical Amplitude Parameters A (\AA), B (\AA^{-1}), and C (\AA^{-1}) and Phase Parameters P_0 , P_1 , P_2 , and P_3 for Atom Pairs $X\text{-}Y = \text{Co-C}$, Co-P , and Co-Co Where X Is the Absorber and Y Is the Backscatterer

	Co-C	Co-P	Co-Co
A	2.122	0.747	0.640
B	0.632	0.240	0.191
C	0.88	3.26	6.66
P_0	2.977	0.205	2.455
P_1	-1.415	-1.345	-1.200
P_2	0.0362	0.0320	0.0253
P_3	27.0	27.0	-59.5

teresting case is the "covering up" of the difference in interatomic distances in a two-term fit by an "apparent larger" Debye-Waller factor in a one-term fit for a one-scatterer two-distance system. This severely limits the resolution of the distance determination to no better than 0.05\AA for a data length of ca. $\Delta k \approx 10 \text{\AA}^{-1}$. An excellent example is our recent EXAFS analysis of rubredoxin and its model compounds.²³ In the second case, it is advantageous to use the difference EXAFS technique in conjunction with Fourier filtering as will be described in this paper (or other variation of it) by first best fitting the dominant term(s) and subtracting it from the observed spectrum followed by (either with or without further Fourier filtering) fitting the difference spectrum with the minor term(s). On the other hand, if the difference in EXAFS amplitude is not sufficiently significant, it is more accurate to refine each term or terms in stages (while holding others fixed). For (3), it is possible to either (a) assume some reasonable Debye-Waller factors (from vibrational data of analogous compounds) in order to determine the coordination numbers or (b) assume certain bond ratios and search for the χ^2 minimum (assuming that the resulting Debye-Waller factors are reasonable). The latter has been successfully applied²² to a number of polymer-bound rhodium catalysts which allows differentiation of various plausible structures based upon the determination of bond ratios which correspond to the minimum χ^2 .

In this paper we employ the recently reported theoretical amplitude and phase functions in the data analysis. These parameterized functions, as well as the number of bonds N_i , are held fixed in all our fitting procedures. The parameterized theoretical amplitude and phase functions are

$$F_i(k_i) = \frac{A_i}{1 + B_i^2(k_i - C_i)^2}$$

and

$$\phi_i(k_i) = P_0 + P_1 k_i + P_2 k_i^2 + P_3/k_i^3$$

where the parameters $\{A, B, C\}$ and $\{P_0, P_1, P_2, P_3\}$ were taken from the literature^{25a,b} and listed in Table I. Since the phase functions are unique only when a particular energy threshold E_0 is specified, our choice of $E_0 = 7750 \text{ eV}$ may not be consistent with the theoretical E_0 's for each of the different types of bonds for which the theoretical phase shift $\phi_i(k_i)$ is defined. We therefore allow a different E_0 value for each type of bond via least-squares refining the difference $\Delta E_{0i}(\text{eV}) = E_{0i}^{\text{th}} - E_0^{\text{exp}}$ in

$$k_i = \sqrt{k^2 - 2(\Delta E_{0i})/7.62}$$

where k is the experimental wavevector with $E_0^{\text{exp}} (= 7750 \text{ eV})$ and k_i is the theoretical wavevector with E_{0i}^{th} . Thus, for $[\text{CpCoPPh}_2]_2$, ten parameters are varied: the overall scale factor N , three Debye-Waller factors σ_C , σ_P , and σ_{Co} , three distances r_C , r_P , and r_{Co} , and three threshold energy differ-

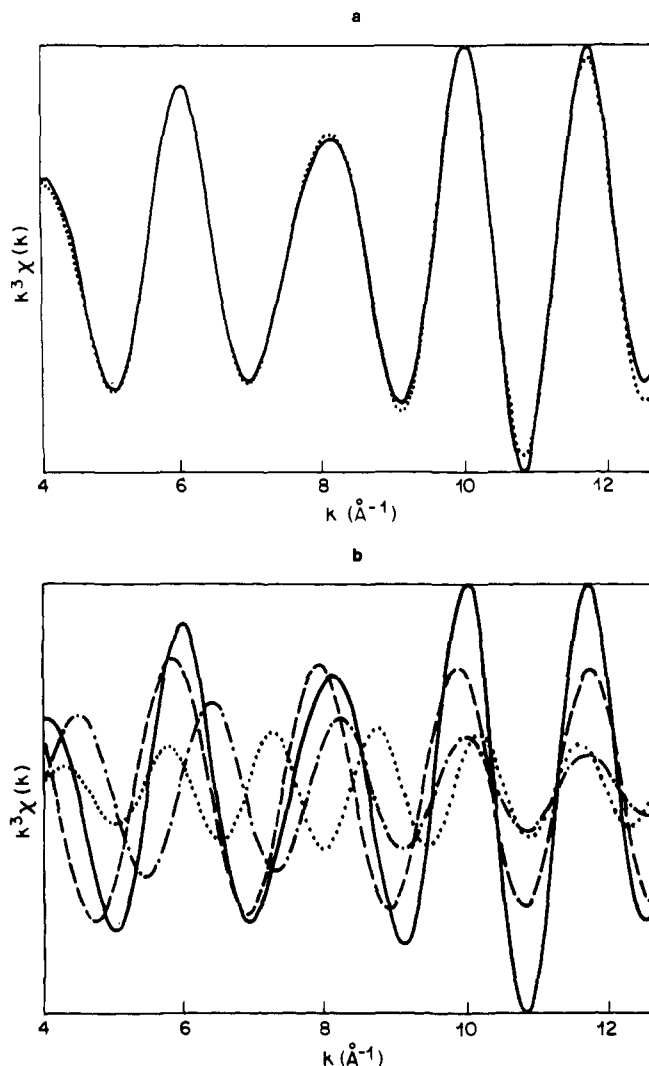


Figure 4. (a) Theoretical fit (dotted curve) of the filtered EXAFS spectrum (solid curve) for $[\text{CpCoPPh}_2]_2$; (b) the three backscattering components in the filtered EXAFS spectrum (---) of $[\text{CpCoPPh}_2]_2$ as resolved by theory: 5C (- - -), 2P (- . . . -), 1Co (\cdots). The ordinate scales are -5.93 to 5.33\AA^{-3} for both (a) and (b).

ences ΔE_{0C} , ΔE_{0P} , and $\Delta E_{0\text{Co}}$. The best fit for $[\text{CpCoPPh}_2]_2$ is shown in Figure 4(a).

For Cp_2Co , there is only one kind of neighboring atoms. The model reduces to one term (first term of eq 3) with four parameters in the least-squares refinement: the overall scale factor N , the Debye-Waller factor σ_C , the Co-C distances r_C , and the threshold energy difference ΔE_{0C} . For the two cationic species 3 and 4, attempts to fit the EXAFS spectra with a three-term model (eq 3) failed to give reasonable σ_{Co} , r_{Co} , and $\Delta E_{0\text{Co}}$ owing to the relatively small magnitude of the single cobalt contribution (as a scatterer) in comparison to that of five cyclopentadienyl carbons and two phosphorus atoms. Even in the neutral parent compound 2, the contributions from the carbon and the phosphorus atoms outweigh that of the cobalt atom, as exemplified in Figure 4(b). Upon oxidation, it is expected that the cobalt-cobalt bond weakens significantly. The resulting increase in Debye-Waller factor σ_{Co} and the increase in Co-Co distance, if any, will further diminish the cobalt contribution to the EXAFS. This effect is evident from the Fourier transform of 2, 3, and 4 shown in Figure 3. For 2, there are two peaks: a stronger one at $r = 1.60 \text{\AA}$ (uncorrected for phase shifts) due to both carbon and phosphorus atoms and a weaker one at $r = 2.11 \text{\AA}$ (uncorrected) due to the cobalt atom. In 3 and 4, the second peak diminishes to about one-half the

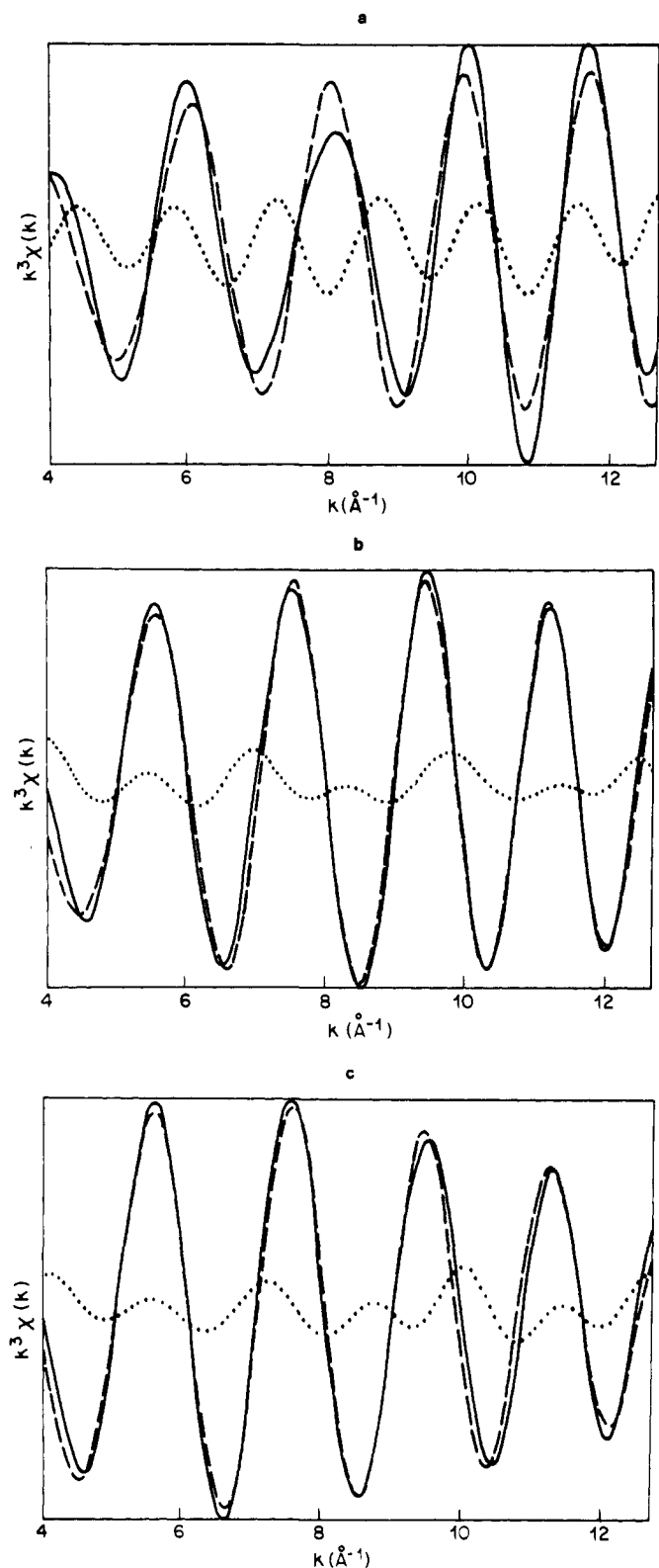


Figure 5. Difference EXAFS spectra (dotted curves) as obtained by subtracting the best fits (dashed curves) with a two-term ($5C + 2P$) model from the filtered data (solid curves): (a) $[\text{CpCoPPh}_2]_2$; (b) $[\text{CpCoPPh}_2]_2^+$; (c) $[\text{CpCoPPh}_2]_2^+ / [\text{CpCoPPh}_2]_2\text{OH}^+$. The ordinate scales are (a) -5.93 to 5.33 ; (b) -5.82 to 5.92 ; and (c) -6.46 to 6.35 \AA^{-3} .

height in **2**, indicating a significant weakening of the Co-Co bond.³¹

To assess the relative strength and the distance of the Co-Co bond in **3** and **4**, we resort to the difference Fourier transform technique.³² It involves first fitting the filtered data with a

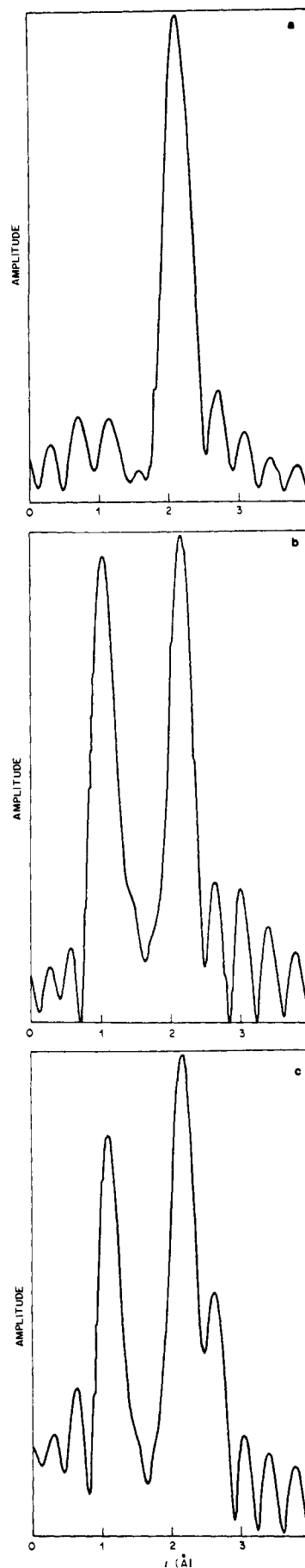


Figure 6. Fourier transforms of the difference EXAFS spectra shown in Figure 5. The ordinate scales are (a) $0-58$; (b) $0-27$; and (c) $0-33 \text{ \AA}^{-4}$.

two-term model which contains the EXAFS contributions from five carbon atoms and two phosphorus atoms (first two terms of eq 3) as shown in Figures 5(a)–(c), for **2**, **3**, and **4** (dashed curves), respectively. The model (5C + 2P) was then subtracted from the data, resulting in a *difference EXAFS spectrum* which presumably contains the cobalt contribution and some residual background not removed by Spline technique or filtered by Fourier filtering. These *difference* spectra are shown also in Figures 5(a)–(c) as dotted curves. The Fourier transforms (Figures 6(a)–(c)) of these difference maps reveal clearly the cobalt contribution(s) as the only discernible feature. Fourier filtering was then performed on these difference spectra with a window of 1.4–3.4 Å to remove the residual background and/or residual contributions, if any, from Co–C and Co–P bonds. The resulting filtered difference spectra were then fitted with a one-term (cobalt) model (except **4**, which requires two different cobalt distances owing to the ca. 2:1 mixture of **3** and **4**) as shown in Figures 7(a)–(c).

The resulting least-squares refined interatomic distances and the Debye–Waller factors (with estimated errors)³³ are tabulated in Table II.

Results

It is evident from Table II that EXAFS spectroscopy can provide accurate structural parameters for noncrystalline solid. For $[\text{CpCoPPh}_2]_2$ and $[\text{CpCoPPh}_2]_2\text{OH}^+$, which have been structurally characterized by the single-crystal x-ray diffraction method, the agreement is exceedingly good. The Co–C distance of 2.094 (2) Å in Cp_2Co determined by EXAFS is significantly greater than the Fe–C distance of 2.064 (6) Å in Cp_2Fe ^{34a} but substantially smaller than the Ni–C distance of 2.196 (8) Å in Cp_2Ni ,^{34b} in accord with the notion that Cp_2Co has one, and Cp_2Ni has two, extra electrons over Cp_2Fe occupying a metal–carbon antibonding orbital.

The two sets of somewhat different bond distances determined from the EXAFS spectrum of $[\text{CpCoPPh}_2]_2$ agree reasonably well with the reported single-crystal x-ray diffraction values. In particular, the Co–C, Co–P, and Co–Co distances of 2.034 (4), 2.169 (19), and 2.572 (9) Å, respectively, obtained by directly fitting the filtered data (cf. Figure 4a), agree very well with the corresponding reported values of 2.046 (20), 2.16 (1), and 2.56 (1) Å.⁹ On the other hand, the difference-Fourier technique gave Co–C, Co–P (fitting the filtered data with Co–C and Co–P contributions only), and Co–Co (fitting the filtered difference map with Co–Co contribution only) distances of 2.054 (43), 2.119 (30), and 2.601 (1) Å, in somewhat worse agreement with the literature results. This phenomenon is readily understandable in that the Co–Co backscattering amplitude in the neutral compound amounts to about 25% (cf. Figure 5(a)) of the overall amplitude and its sinusoidal function ($\sin(2kr_{\text{Co}} + \phi_{\text{Co}}(k))$) is not completely orthogonal to those of the carbon and the phosphorus atoms³⁵ such that ignoring it will lead to errors in Co–C and Co–P distances in the initial fitting which subsequently lead to an error in the Co–Co distance in the difference map. For the charged species, the EXAFS contribution from the cobalt scattering is substantially less owing to the significant increase in Debye–Waller factor as a result of the weakening in metal–metal bond (ca 15%; cf. Figures 5(b) and (c)). We expect a better fit with just Co–C and Co–P contributions and therefore more accurate bond distances for these systems via the difference-Fourier technique.

For the monocationic species $[\text{CpCoPPh}_2]_2^+$, we determined the Co–C, Co–P, and Co–Co distances to be 2.071 (6), 2.223 (9), and 2.649 (4) Å, respectively. For the mixture of $[\text{CpCoPPh}_2]_2^+$ and $[\text{CpCoPPh}_2]_2\text{OH}^+$ (ca. 2:1), we found Co–C and Co–P at 2.051 (8) and 2.226 (6) Å, respectively, and two Co–Co distances of 2.644 (1) (due to $[\text{CpCoPPh}_2]_2^+$) and

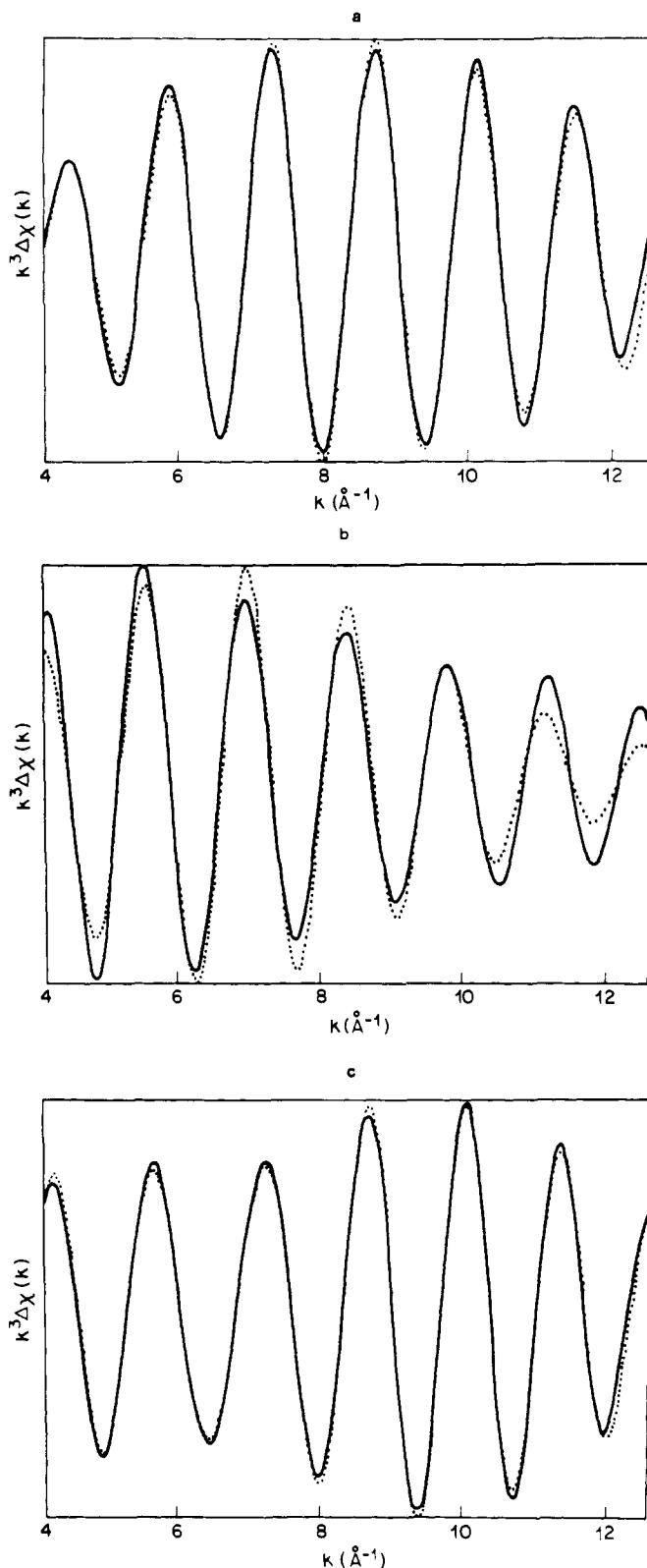


Figure 7. Theoretical fits (dotted curves) of the Fourier filtered (solid curves) difference EXAFS spectra from Figures 5 and 6 with cobalt contributions only: (a) $[\text{CpCoPPh}_2]_2$, single distance; (b) $[\text{CpCoPPh}_2]_2^+$, single distance; (c) $[\text{CpCoPPh}_2]_2^+ / [\text{CpCoPPh}_2]_2\text{OH}^+$, two distances. The ordinate scales are (a) -1.29 to 1.28 ; (b) -0.61 to 0.61 ; and (c) -0.77 to 0.75 \AA^{-3} .

2.884 (1) Å (due to $[\text{CpCoPPh}_2]_2\text{OH}^+$). The Co–C, Co–P, and Co–Co distances in the structurally characterized $[\text{CpCoPPh}_2]_2\text{OH}^+$ are 2.078, 2.213 (6), and 2.901 (5) Å, respectively.⁸ It should be mentioned that in our EXAFS anal-

Table II. The Least-Squares Refined Interatomic Distances (Å) and Debye-Waller Factors (Å) with Fitting Errors (Excluding Systematic Errors Such as Background Removal, Fourier Filtering, and Difference-Fourier Analysisⁱ Which Amount to ca. 0.5% in r and 10% in σ)

	Co-C		Co-P		Co-Co	
	r	σ	r	σ	r	σ
Cp ₂ Co ^a	2.094 (2)	0.057 (6) ^a				
[CpCoPPh ₂] ₂ ^b	2.034 (4)	0.000 (17) ⁱ	2.169 (19)	0.072 (15)	2.572 (9)	0.058 (4)
[CpCoPPh ₂] ₂ ^c	2.054 (43) ^c	0.004 (53) ^{c,i}	2.119 (30) ^c	0.030 (55) ^c	2.601 (1) ^d	0.066 (1) ^d
[CpCoPPh ₂] ₂ ⁺	2.071 (6) ^e	0.028 (17) ^{e,i}	2.223 (9) ^e	0.001 (26) ^e	2.649 (4) ^f	0.100 (2) ^f
[CpCoPPh ₂] ₂ OH ⁺	2.051 (8) ^g	0.000 (45) ^{g,i}	2.226 (6) ^g	0.013 (25) ^g	2.884 (1) ^h	0.082 (1) ^h
					2.644 (1) ^h	0.095 (1) ^h

^a Fit with data truncated at 5 and 12.6 Å⁻¹ (cf. Figure 2a). ^b Fit with a three-term (5C + 2P + 1Co) model (cf. Figure 4a). ^c Fit with a two-term (5C + 2P) model (cf. Figure 5a). ^d Fitting of the difference EXAFS spectrum (cf. Figure 7a) with cobalt contribution only. ^e Fit with a two-term (5C + 2P) model (cf. Figure 5b). ^f Fitting of the difference EXAFS spectrum (cf. Figure 7b) with cobalt contribution only. ^g Fit with a two-term (5C + 2P) model (cf. Figure 5c). ^h Fitting of the difference EXAFS spectrum (cf. Figure 7c) with two Co-Co distances. ⁱ The near-zero values for the Debye-Waller factors of the Co-C bonds is an artifact of the theoretical backscattering amplitude for light scatterers with atomic number <9 and therefore should not be taken seriously.^{25a} ^j The error due to the difference-Fourier technique depends on the degree of nonorthogonality of various backscattering terms.³⁵ For the present systems, the r and σ values determined by this technique could be in error by 2 and 20%, respectively.

ysis, we ignore the backscattering from the bridging OH group in [CpCoPPh₂]₂OH⁺ for simplicity. Inclusion of the effect of the OH group by assuming six Co-C contributions (this is a reasonable assumption since the covalent radii and the atomic numbers of carbon and oxygen are quite alike) did not change the resulting distances by more than one standard deviation.

If we assume that the number of cobalt-cobalt bonds in [CpCoPPh₂]₂ is one ($N_{Co} = 1$), then calibrations based upon the overall scale factor (N) of the two-term fit (5C + 2P) and the difference fit (Co) give rise to reasonable N_{Co} values of 0.89 in [CpCoPPh₂]₂⁺ and 0.86 in the [CpCoPPh₂]₂⁺/[CpCoPPh₂]₂OH⁺ mixture. The departure of the latter values from the expected value of one is to a significant extent due to the somewhat chemical (bonding) sensitivity of the amplitude parameter A . Nevertheless, the utility of EXAFS spectroscopy in predicting coordination numbers is well illustrated.

The most striking result of this work is the relatively small increase of 0.08 Å in the metal-metal distance in going from the neutral compound (2.57 Å) to its monocation (2.65 Å). From the nonparameterized molecular orbital (MO) calculations performed on the structurally analogous and electronically equivalent Fe₂(CO)₆X₂ systems,^{2b} we expect the highest occupied MO (HOMO) of [CpCoPPh₂]₂ to be highly bonding between the two cobalt atoms.

Furthermore, the characteristic well-resolved 31-line EPR spectrum of the monocation has been interpreted as hyperfine interactions due to two equivalent cobalt nuclei of $I = 7/2$ (splitting into 15 lines of intensities 1:2:3 . . . 8 . . . 3:2:1) with $a_{Co} = 22.66$ G and two equivalent phosphorus nuclei of $I = 1/2$ (each further split into a 1:2:1 triplet) with $a_P = 11.33$ G, suggesting that the HOMO is indeed primarily cobalt in character.⁸ Assuming no drastic reordering of the electronic structure upon oxidation, this would then predict a significant weakening in the metal-metal bonding interaction, and thus a lengthening of the metal-metal distance, when one electron is moved from the HOMO of the neutral species. Indeed, the metal-metal distance increases by 0.08 Å. The magnitude of this increment, however, is much smaller than that observed in the metal-metal nonbonded ($n = 0$) [CpFe(CO)PPh₂]₂ⁿ ($n = 0, +1, +2$) series, albeit significantly greater than that observed in the metal-metal bonded ($n = 0$) [CpMo(SMe)₂]₂ⁿ ($n = 0, +1$) series (vide infra).

There is no doubt that upon one-electron oxidation, the cobalt-cobalt bond in [CpCoPPh₂]₂ weakens substantially. This is evident from the drastic increase in the Debye-Waller factor, going from 0.058 (4) Å in the neutral to 0.100 (2) Å in the monocation. Granting the reasonable assumption that no drastic structural change occurs upon oxidation, the ratio of the metal-metal force constant of the two systems can be es-

timated by using the equation^{36a}

$$\sigma^2 = (h/8\pi^2\mu\nu) \coth(h\nu/2kT)$$

where μ is the reduced mass, T is the temperature, and ν is the vibrational frequency. Assuming that the metal framework can be treated as a diatomic system (viz., $K = 4\pi^2\mu\nu^2$ and $\mu \approx 29.5$ where K is the metal-metal vibrational force constant) we estimate $K_0 = 1.40$ mdyn/Å ($\sigma = 0.058$ Å) or 1.07 mdyn/Å ($\sigma = 0.066$ Å) and $K_+ = 0.43$ mdyn/Å ($\sigma = 0.100$ Å) for the neutral species and the monocation, respectively, resulting in a K_0/K_+ ratio of 2.5-3.3. Alternatively, it can be argued that for weak chemical bonds or at the high-temperature limit $h\nu \ll kT$, σ is proportional to $\sqrt{T/K}$, thereby giving rise to $K_0/K_+ \approx 3.0$ for $\sigma_+/\sigma_0 \approx \sqrt{3}(0.100/0.058)$. It should be emphasized that despite the fact that the force constants are quite reasonable (e.g., the Fe-Fe force constant in the structurally analogous Fe₂(CO)₆S₂ system was estimated to be 1.29 mdyn/Å by a detailed vibrational analysis^{36b}), the absolute values of these force constants should be treated with caution owing to the crude diatomic approximation invoked. On the other hand, we believe that the ratio of $K_0/K_+ = 3.0 \pm 0.5$ is a reliable indication that the metal-metal stretching force constant decreases, and hence the metal-metal bond weakens, significantly upon one-electron oxidation. We believe that this is consistent only with the premise that the electron being removed comes from an orbital which is highly bonding between the two cobalt atoms.

Discussion

It is now apparent that metal-metal distance per se does not indicate the strength of metal-metal bonding. We consider next the effects of changing the overall structure, the bridging atoms (B), the substituents on the bridging atoms (R), the terminal ligands (Y), the metal atoms (M), and, finally, the number of valence electrons on the metal-metal distances in a number of dimeric metal clusters.

First, consider, for example, the metal-metal distances in Fe₂(NO)₄(SEt)₂,^{37a} Fe₂(CO)₆(SEt)₂,^{37b} and *cis*-[Cp₂Fe₂(CN)₂(SEt)₂]^{37c}—each with a distinctly different structure but similar Fe₂(μ₂-S)₂ linkages. The *single* Fe-Fe bond lengths in these species are 2.720 (3), 2.537 (10), and 2.625 (3) Å, respectively, which bear no obvious relationship to the iron formal oxidation states of 0, I, and III, respectively. It is obviously impossible to deduce the degree of metal-metal bonding from metal-metal distance alone when different structures are involved.

Second, consider the effect of bridging atoms on metal-metal distance in, e.g., (1) Fe₂(NO)₄(SEt)₂ (2.720 (3) Å) vs. Fe₂(NO)₄I₂ (3.05 (1) Å),^{37d} (2) Fe₂(CO)₆(NH₂)₂ (2.402 (6)

Table III. Comparison of Mean Geometrical Parameters for Some Representative Metal Dimers^a with Varying Number of Metal Cluster Electrons

Complex	Bond order	M-M	M-B	Ref
[CpNiPPh ₂] ₂	0	3.36 (1)	2.15 (0.8)	9
[CpCoPPh ₂] ₂	1	2.56 (1)	2.16 (0.8)	9
[CpCoPPh ₂] ₂ ⁺	0.5	2.649 (4)	2.223 (9)	This work
[CpMo(SMe) ₂] ₂	1	2.603 (2)	2.46	6
[CpMo(SMe) ₂] ₂ ⁺	?	2.617 (4)	2.44	6
[CpFe(CO)PPh ₂] ₂	0	3.498 (4)	2.261 (6)	3
[CpFe(CO)PPh ₂] ₂ ⁺	0.5	3.14 (2)	2.22 (3)	3
[CpFe(CO)PPh ₂] ₂ ²⁺	1	2.764 (4)	2.236 (7)	3
[CpFe(CO)SPh] ₂	0	3.39	2.262 (6)	4a
[CpFe(CO)SMe] ₂ ⁺	0.5	2.925 (4)	2.234 (4)	4b
[CpFe(NCCH ₃)SEt] ₂ ²⁺	1	2.649 (7)	2.205 (5)	4c
[CpNi(CO)] ₂	1	2.36		39a
[CpCo(CO)] ₂ ⁻	1.5	2.36	1.83	39b
[CpFe(NO)] ₂	2	2.324 (2)	1.778 (5)	39c
Co ₂ (CO) ₆ (C ₂ (<i>t</i> -Bu) ₂)	1	2.463 (1)	1.996 (4)	40
Fe ₂ (CO) ₆ (C ₂ (<i>t</i> -Bu) ₂)	2	2.316 (1)	2.082 (7)	40
Fe ₂ (CO) ₄ (C ₂ (<i>t</i> -Bu) ₂)	2	2.215	2.082	41a
Fe ₂ (CO) ₄ (C ₂ R ₂ S) ₂	2	2.225 (3)	2.054	41b
Cb ₂ Fe ₂ (CO) ₃	3	2.177 (3)	1.974	42a
[MeCpCr(CO)] ₂	3	2.276 (2)		42b

^a Cp = $\eta^5\text{-C}_5\text{H}_5$, Ph = C₆H₅, Me = CH₃, Et = C₂H₅, C₂(*t*-Bu)₂ = 2,2,5,5-tetramethylhex-3-yne, C₂R₂S = 3,3,6,6-tetramethyl-1-thiacyclohept-4-yne, Cb = $\eta^4\text{-1,2-diphenyl-3,4-di-}i\text{-tert-butylcyclobutadiene}$, MeCp = $\eta^5\text{-pentamethylcyclopentadienyl}$.

Å)^{37e} vs. Fe₂(CO)₆(PPh₂)₂^{37f} (2.623 (2) Å) vs. Fe₂(CO)₆(SPh)₂ (2.516 (2) Å),^{37g} (3) Fe₂(CO)₉ (2.523 (1) Å)^{37h} vs. Fe₂(CO)₆(CO)(GePh₂)₂ (2.666 (3) Å)³⁷ⁱ vs. Fe₂(CO)₆(GeMe₂)₃ (2.75 (1) Å).^{37j} The Fe-Fe bond in each of these species (with identical structures and similar terminal ligands) is formally of bond order one, yet the Fe-Fe distance ranges from 2.40 to 3.05 Å owing to the different covalent radii of the bridging atoms.

Third, consider the effect imposed by the substituents of the bridging atoms. The obvious examples are Fe₂(CO)₆(PR₂)₂, where the *single* Fe-Fe bond lengths range from 2.623 (3) in R = Ph^{37f} to 2.665 (2) in R = Me^{37f} to 2.819 (1) Å in R = CF₃.^{37k} The corresponding Fe-P distances decrease in the order 2.233 (3) > 2.209 (2) > 2.193 (1) Å. The surprisingly long Fe-Fe bond in the latter compound is believed to be caused by the strong electron-withdrawing CF₃ substituents on the bridging phosphorus atoms which favor larger Fe-P-Fe bridging angles.^{37k}

Fourth, the effect of terminal ligands can be illustrated by contrasting Fe₂(NO)₄(SEt)₂ (2.720 (3) Å) vs. [Fe₂(SR)₄S₂]²⁻ (R = tolyl, 2.691 (1) Å; (SR)₂ = xylyl, 2.698 (1) Å) vs. Cp₂Fe₂(CN)₂(SEt)₂ (2.625 (3) Å).

It is apparent from the foregoing discussions that the metal-metal distance for a given bond order in a metal dimer is to a large extent dictated by the stereochemical constraints and electronic effects imposed by the ligands (in addition to local metal coordination and metal-metal interactions). No simple correlation can be drawn between the interatomic distance and the degree of bonding interaction between the metal atoms.⁷

We consider next the effect of varying the number of valence electrons available for metal-metal interaction (hereafter referred to as "metal cluster electrons") in some representative metal dimers, including the title compounds. The pertinent structural data are summarized in Table III. Since metal-metal interactions are in general much weaker than metal-ligand interactions, the metal-ligand bonding orbitals often

lie lower, whereas the metal-ligand antibonding orbitals often lie higher, in energy than the "metal cluster orbitals" which are predominantly metal in character and responsible for the metal-metal interactions.^{2b} Therefore, any perturbation in valence band via redox or substitution of the metal atom(s) or the ligand(s) will most likely affect the metal cluster electronic configuration more than it affects the metal-ligand bonds.

The most common examples in the stereochemical controls of metal cluster electrons are those involving the highly *antibonding* metal cluster orbitals. Removal (addition) of valence electrons from (to) these molecular orbitals via redox reaction or metal or ligand substitution generally causes drastic decreases (increases) in metal-metal distance. A beautiful example is the stepwise one-electron oxidation of [CpFe(CO)PPh₂]₂ to give the mono- and dicationic species. Structural characterizations revealed a stepwise decrease of the Fe-Fe distance from a nonbonding value of 3.498 (4) Å in the neutral to a half-bonding value of 3.14 (2) Å in the monocation to a bonding value of 2.764 (4) Å in the dication. This systematic variation in the metal-metal separation among closely related species has been taken as strong evidence that the electron(s) are being removed from a highly metal-metal antibonding orbital. MO calculations³⁸ suggest metal cluster electronic configurations of $\sigma^2\pi^2\delta^2\delta^*2\pi^*2\sigma^*n$ where $n = 2, 1, \text{ and } 0$, resulting in a metal-metal bond order of 0, 0.5, and 1 for the neutral, mono-, and dicationic species, respectively. Similar arguments apply to the series [CpFe(CO)SPh]₂, [CpFe(CO)SMe]₂⁺, and [CpFe(NCCH₃)SEt]₂²⁺ where the Fe-Fe distance decreases from 3.39 to 2.925 (4) to 2.649 (7) Å, respectively. Further removal of antibonding π -type metal cluster electron(s) can result in a further reduction of metal-metal separation. A good example is the series [CpNi(CO)]₂,^{39a} [CpCo(CO)]₂⁻,^{39b} and [CpFe(NO)]₂,^{39c} which have metal-metal distances of 2.36, 2.36, and 2.324 (2) Å, respectively. Taking into consideration the difference in covalent radii of Ni (1.15 Å) vs. Co (1.16 Å) vs. Fe (1.17 Å) and C (0.77 Å) vs. N (0.75 Å), the effective reduction in metal-metal separation amounts to ca. 0.02–0.03 Å in going from the nickel to the cobalt to the iron system. These latter decreases in metal-metal distance are consistent with the removal of one and two electrons from the π -type antibonding metal cluster orbitals, resulting in bond orders of 1, 1.5, and 2 for [CpNi(CO)]₂, [CpCo(CO)]₂⁻, and [CpFe(NO)]₂, respectively. Another beautiful example is the isostructural series M₂(CO)₆[C₂(*t*-Bu)₂]₂ (M = Co, Fe) which have metal-metal distances of 2.463 (1) and 2.316 (1) Å for M = Co and Fe, respectively. The dicobalt cluster is structurally analogous and electronically equivalent (in a formal sense) to [CpCoPPh₂]₂, each possessing a single cobalt-cobalt bond. Formal removal of two valence electrons from Co₂(CO)₆[C₂(*t*-Bu)₂]₂ to give the diiron cluster, in contrast to the title compound, results in a shortening (0.14 Å) and presumably strengthening of the metal-metal bond to form an iron-iron double bond.⁴⁰ This is consistent only with the notion that the highest occupied MO in Co₂(CO)₆[C₂(*t*-Bu)₂]₂ is of pseudo- π -type antibonding character (2a₂ in Figure 2 of ref 2b). Further removal of two more antibonding metal cluster electrons results in metal-metal triple bonds; examples include the triply bridged (Ph₂(*t*-Bu)₂C₄)₂Fe₂(CO)₃^{42a} ($a_1'^2a_2'^2e'^4e'^4e'^0a_2'^0$), which has a Fe≡Fe distance of 2.177 (3) Å, and the nonbridged [($\eta^5\text{-Me}_5\text{C}_5$)Cr(CO)]₂,^{42b} which has a Cr≡Cr distance of 2.276 (2) Å.

The effect of removing (adding) an electron from (to) a highly *bonding* metal cluster orbital on the metal-metal distance is relatively unknown. In fact, to the best of our knowledge, this work represents the first structural characterization of a "genuine" one-electron metal-metal bond where one electron is removed from a highly bonding metal cluster orbital (5a₁ in Figure 2 of ref 2b, assuming that [CpCoPPh₂]₂ is

electronically analogous to $\text{Fe}_2(\text{CO})_6\text{X}_2$ systems^{2b}). The most striking result is the two- to threefold reduction in the metal-metal stretching force constant in going from $[\text{CpCoPPh}_2]_2$ (bond order of one) to $[\text{CpCoPPh}_2]_2^+$ (bond order of 0.5). Surprisingly, however, the Co-Co distance *increases* by only 0.08 Å, in sharp contrast to the drastic *decrease* of 0.8 Å in the metal-metal distance when two electrons are removed (formally) from the highly *antibonding* metal cluster orbital in $[\text{CpNiPPh}_2]_2$ to form $[\text{CpCoPPh}_2]_2^+$.⁹ On the other hand, this small increase of 0.08 Å in metal-metal distance observed for a one-electron oxidation of the metal-metal bonded dimer $[\text{CpCoPPh}_2]_2$ is significantly greater than the increase of only 0.014 Å observed in the one-electron oxidation of the Mo-Mo bonded $[\text{CpMo}(\text{SMe})_2]_2$ to its monocation. For the latter system, however, no other evidence is available as to whether the Mo-Mo single bond in the neutral species actually weakens, strengthens, or is unchanged (which corresponds to removal of an electron from bonding, antibonding, and non-bonding metal cluster orbitals, respectively) upon the one-electron oxidation.

In conclusion, it is conceivable that the stereochemical influence on the metal framework imposed by varying the number of electrons in metal cluster orbitals decreases drastically in going from antibonding to bonding to (or) non-bonding orbitals (with respect to metal-metal interactions).

Acknowledgments. We thank Dr. P. A. Lee for valuable consultations and A. L. Simons for the least-squares refinement routines utilized in this work. We are also grateful to Drs. J. D. Sinclair and R. G. Shulman for helpful discussions. The authors are indebted to Dr. H. Winick and other SSRL staff members for their technical assistance. Synchrotron radiation was provided by the Stanford Synchrotron Radiation Laboratory, supported by National Science Foundation Grant DMR73-07692 in cooperation with the Stanford Linear Accelerator Center and the Energy Research and Development Administration.

References and Notes

- (1) (a) For previous papers in this series, see B. K. Teo and J. C. Calabrese, *Inorg. Chem.*, **15**, 2467, 2474 (1976); (b) Trinh-Toan, W. P. Fehlhammer, and L. F. Dahl, *J. Am. Chem. Soc.*, **99**, 402 (1977); (c) Trinh-Toan, B. K. Teo, J. A. Ferguson, T. J. Meyer, and L. F. Dahl, *ibid.*, **99**, 408 (1977).
- (2) (a) B. K. Teo, M. B. Hall, R. F. Fenske, and L. F. Dahl, *J. Organomet. Chem.*, **70**, 413 (1974); (b) *Inorg. Chem.*, **14**, 3103 (1975).
- (3) J. D. Sinclair, Ph.D. Thesis, University of Wisconsin, Madison, Wis., 1972.
- (4) (a) G. Ferguson, C. Hannaway, and K. M. K. Islam, *Chem. Commun.*, 1165 (1968); (b) N. G. Connelly and L. F. Dahl, *J. Am. Chem. Soc.*, **92**, 7472 (1970); (c) P. J. Vergamini, G. J. Kubas, and R. R. Ryan, private communication.
- (5) (a) R. E. Dessy, A. L. Rheingold, and G. D. Howard, *J. Am. Chem. Soc.*, **94**, 746 (1972); (b) R. E. Dessy, R. Kornmann, C. Smith, and R. Haytor, *ibid.*, **90**, 2001 (1968); (c) R. E. Dessy and L. A. Bares, *Acc. Chem. Res.*, **5**, 415 (1972).
- (6) N. G. Connelly and L. F. Dahl, *J. Am. Chem. Soc.*, **92**, 7470 (1970).
- (7) R. H. Summerville and R. Hoffmann, *J. Am. Chem. Soc.*, **98**, 7240 (1976).
- (8) B. K. Teo, Ph.D. Thesis, University of Wisconsin, Madison, Wis., 1973, Chapter II.
- (9) J. M. Coleman and L. F. Dahl, *J. Am. Chem. Soc.*, **89**, 542 (1967).
- (10) (a) R. G. Hayter, *Inorg. Chem.*, **2**, 1031 (1963); (b) R. G. Hayter and L. F. Williams, *J. Inorg. Nucl. Chem.*, **26**, 1977 (1964).
- (11) E. A. Stern, *Phys. Rev. Sect. B*, **10**, 3027 (1974).
- (12) C. A. Ashley and S. Doniach, *Phys. Rev. Sect. B*, **11**, 1279 (1975).
- (13) P. A. Lee and J. B. Pendry, *Phys. Rev. Sect. B*, **11**, 2795 (1975).
- (14) P. A. Lee and G. Beni, *Phys. Rev. Sect. B*, **15**, 2862 (1977).
- (15) B. M. Kincaid and P. Eisenberger, *Phys. Rev. Lett.*, **34**, 1361 (1975).
- (16) D. E. Sayers, F. W. Lytle, and E. A. Stern, *Adv. X-Ray Anal.*, **13**, 248 (1970).
- (17) (a) D. E. Sayers, E. A. Stern, and F. W. Lytle, *Phys. Rev. Lett.*, **27**, 1204 (1971); (b) F. W. Lytle, D. E. Sayers, and E. A. Stern, *Phys. Rev. Sect. B*, **11**, 4825 (1975); (c) E. A. Stern, D. E. Sayers, and F. W. Lytle, *ibid.*, **11**, 4836 (1975), and references cited therein.
- (18) (a) D. E. Sayers, E. A. Stern, and F. W. Lytle, *Phys. Rev. Lett.*, **35**, 584 (1975); (b) D. E. Sayers, F. W. Lytle, M. Weissbluth, and P. Pianetta, *J. Chem. Phys.*, **62**, 2514 (1975); (c) F. W. Lytle, D. E. Sayers, and E. B. Moore, Jr., *Appl. Phys. Lett.*, **24**, 45 (1974).
- (19) P. H. Citrin, P. Eisenberger, and B. M. Kincaid, *Phys. Rev. Lett.*, **36**, 1346 (1976).
- (20) S. P. Cramer, T. K. Eccles, F. Kutzler, K. O. Hodgson, and S. Doniach, *J. Am. Chem. Soc.*, **98**, 8059 (1976).
- (21) R. G. Shulman, P. Eisenberger, W. E. Blumberg, and N. A. Stombaugh, *Proc. Natl. Acad. Sci. U.S.A.*, **72**, 4003 (1975).
- (22) J. Reed, P. Eisenberger, B. K. Teo, and B. M. Kincaid, *J. Am. Chem. Soc.*, **99**, 5217 (1977).
- (23) R. G. Shulman, P. Eisenberger, B. K. Teo, B. M. Kincaid, and G. S. Brown, *Biochemistry*, in press.
- (24) (a) B. M. Kincaid, P. Eisenberger, K. O. Hodgson, and S. Doniach, *Proc. Natl. Acad. Sci. U.S.A.*, **72**, 2340 (1975); (b) P. Eisenberger and B. M. Kincaid, *Chem. Phys. Lett.*, **36**, 134 (1975); (c) P. Eisenberger, R. G. Shulman, G. S. Brown, and S. Ogawa, *Proc. Natl. Acad. Sci. U.S.A.*, **73**, 491 (1976).
- (25) (a) B. K. Teo, P. A. Lee, A. L. Simons, P. Eisenberger, and B. M. Kincaid, *J. Am. Chem. Soc.*, **99**, 3854 (1977); (b) P. A. Lee, B. K. Teo, and A. L. Simons, *ibid.*, **99**, 3856 (1977); (c) B. K. Teo, K. Kijima, and R. Bau, *ibid.*, **100**, 621 (1978).
- (26) H. Winick in "Proceedings of the IXth International Conference on High Energy Accelerators", Stanford Linear Accelerator Center, Stanford, Calif., 1974, pp 685-688.
- (27) (a) P. Eisenberger, B. Kincaid, S. Hunter, D. Sayers, E. A. Stern, and F. Lytle in "Proceedings of the Fourth International Conference on Vacuum Ultraviolet Radiation Physics", B. E. Koch, R. Haensel, and C. Kunz, Ed., Pergamon Press, Oxford, pp 806-807; (b) B. M. Kincaid, P. Eisenberger, and D. E. Sayers, to be published.
- (28) (a) A local cubic spline background removal program; (b) a local Fourier filtering routine developed by B. M. Kincaid. Application of Fourier filtering technique to EXAFS analysis has been done independently by Stern, Sayers, and Lytle.^{17c}
- (29) "International Tables for X-Ray Crystallography", Vol. III, Kynoch Press, Birmingham, England, 1968, pp 161, 171.
- (30) D. W. Marquardt, *J. Soc. Ind. Appl. Math.*, **11**, 443 (1963).
- (31) The small peak at $k \approx 1 \text{ \AA}^{-1}$ is due to either truncation of the $k^3\chi(k)$ data (i.e., finite data set) and/or residual background. It is certainly not a real distance since all distances are well above 2 Å which corresponds to $\geq 1.5 \text{ \AA}$ in the Fourier transform. The minor "amplitude disagreement" between the filtered and the raw data (cf. Figure 2) is due to the same reason. It is exactly for this reason that we use a shorter data length ($k = 4-12.6 \text{ \AA}^{-1}$) after Fourier filtering. It does not affect the Debye-Waller factor or our conclusion to any significant extent since the latter affects mainly the larger k region.
- (32) A different "difference fourier analysis" technique has been described in ref 20.
- (33) For one-term fits, the fitting error for each parameter is calculated by changing that particular parameter (while least-squares refining the others) until the χ^2 doubled. For multiterm fits, a procedure similar to one-term fits is followed except that terms other than the one under consideration are held constant and the doubling of χ^2 refers to the χ^2 contribution from that particular term only.
- (34) (a) A. Haaland and J. E. Nilsson, *Acta Chem. Scand.*, **22**, 2653 (1968); (b) L. Hedberg and K. Hedberg, *J. Chem. Phys.*, **53**, 1228 (1970).
- (35) For the two different procedures to give identical results, the cobalt contribution to the EXAFS spectrum must be perfectly orthogonal to those of the carbon and the phosphorus atoms.
- (36) (a) S. J. Cyryn, "Molecular Vibrations and Mean Square Amplitudes", Elsevier, Amsterdam, 1968, p 77; (b) W. M. Scovell and T. G. Spiro, *Inorg. Chem.*, **13**, 304 (1974).
- (37) (a) J. T. Thomas, J. H. Robertson, and E. G. Cox, *Acta Crystallogr.*, **11**, 599 (1958); (b) L. F. Dahl and C. H. Wel, *Inorg. Chem.*, **2**, 328 (1963); (c) P. J. Vergamini, G. J. Kubas, and R. R. Ryan, private communication; (d) L. F. Dahl, E. Rodulfo de Gil, and R. D. Feltham, *J. Am. Chem. Soc.*, **91**, 1653 (1969); (e) L. F. Dahl, W. R. Costello, and R. B. King, *ibid.*, **90**, 5422 (1968); (f) J. Huntsman and L. F. Dahl, to be published; (g) W. Henslee and R. E. Davis, *Cryst. Struct. Commun.*, **1**, 403 (1972); (h) F. A. Cotton and J. M. Troup, *J. Chem. Soc., Dalton Trans.*, 800 (1974); (i) M. Elder, *Inorg. Chem.*, **8**, 2703 (1969); (j) M. Elder and D. Hall, *ibid.*, **8**, 1424 (1969); (k) W. Clegg, *ibid.*, **15**, 1609 (1976); (l) J. J. Maysle, S. E. Denmark, B. V. Depamphilis, J. A. Ibers, and R. H. Holm, *J. Am. Chem. Soc.*, **97**, 1032 (1975).
- (38) C. Campana, Ph.D. Thesis, University of Wisconsin, Madison, Wis., 1975.
- (39) (a) A. A. Hock and O. S. Mills, "Advances in the Chemistry of Coordination Compounds", S. Kirschner, Ed., Macmillan, New York, N.Y., 1961, p 647; (b) N. E. Schore, C. S. Iler, and R. G. Bergman, *J. Am. Chem. Soc.*, **98**, 256 (1976); (c) J. L. Calderon, S. Fortana, E. Frauendorfer, V. W. Day, and S. D. A. Iske, *J. Organomet. Chem.*, **64**, C16 (1974).
- (40) F. A. Cotton, J. D. Jamerson, and B. R. Stults, *J. Am. Chem. Soc.*, **98**, 1774 (1976).
- (41) (a) K. Nicholas, L. S. Bray, R. E. Davis, and R. Pettit, *Chem. Commun.*, 608 (1971); (b) H.-J. Schmitt and M. L. Ziegler, *Z. Naturforsch. B*, **28**, 508 (1973).
- (42) (a) S.-I. Murahashi, T. Mizoguchi, T. Hosokawa, I. Moritani, Y. Kai, M. Kohara, N. Yasuoka, and N. Kasai, *J. Chem. Soc., Chem. Commun.*, 563 (1974); (b) J. Potenza, P. Giordano, D. Mastropaolo, A. Efraty, and R. B. King, *ibid.*, 1333 (1972).